# Orientation-Dependent $C_{60}$ Electronic Structures Revealed by Photoemission Spectroscopy

V. Brouet,[1,2,3] W. L. Yang,[1,2] X. J. Zhou,[2] H. J. Choi,[4,5] S. G. Louie,[4,6] M. L. Cohen,[4,6] A. Goldoni,[7] F. Parmigiani,[7] Z. Hussain,[1] and Z. X. Shen[2]

[1]*Advanced Light Source, Lawrence Berkeley National Laboratory, Berkeley, California 94720, USA*
[2]*Stanford Synchrotron Radiation Laboratory and Department of Applied Physics, Stanford University, Stanford, California 94305, USA*
[3] *Laboratoire de Physique des Solides, Université Paris-Sud, Bât 510, UMR 8502, 91405 Orsay, France*
[4]*Department of Physics, University of California at Berkeley, Berkeley, California 94720, USA*
[5]*Korea Institute for Advanced Study, 207-43 Cheongryangri Dongdaemun, Seoul 130-722, Korea*
[6]*Materials Science Divisions, Lawrence Berkeley National Laboratory, Berkeley, California 94720, USA*
[7]*Sincrotone Trieste S.C.p.A., Strada Statale 14 Km 163.5, Basovizza, 34012 Trieste, Italy*

(Received 17 December 2003; published 5 November 2004)

We observe, with angle-resolved photoemission, a dramatic change in the electronic structure of two $C_{60}$ monolayers, deposited, respectively, on Ag (111) and (100) substrates, and similarly doped with potassium to half filling of the $C_{60}$ lowest unoccupied molecular orbital. The Fermi surface symmetry, the bandwidth, and the curvature of the dispersion at $\Gamma$ point are different. Orientations of the $C_{60}$ molecules on the two substrates are known to be the main structural difference between the two monolayers, and we present new band-structure calculations for some of these orientations. We conclude that orientations play a key role in the electronic structure of fullerides.

DOI: 10.1103/PhysRevLett.93.197601 PACS numbers: 79.60.Jv, 71.28.+d, 73.21.–b, 79.60.Fr

In a standard formulation of quantum theory of solids, the emphasis is on the periodic nature of the lattice structure and the internal degrees of freedom are usually ignored. As the frontier of condensed matter physics moves to more complex solids, such issues become more and more important. In fullerides, electron-electron and electron-phonon interactions are competing on similar energy scales, which challenges standard approximations of solid state physics [1]. Moreover, they are archetypical molecular systems and many degrees of freedom associated with the $C_{60}$ molecule (e.g., vibrational modes, Jahn-Teller distortions, orientational order, etc.) play an important role. A higher sensitivity to local scale structures is in fact typically to be expected in a strongly correlated material, because of the reduced hopping rate.

We reveal here an extreme sensitivity of the band structure of $C_{60}$ monolayers to one of this internal degree of freedom, namely, the molecular orientations. The role of orientations in the electronic properties of fullerides has often been questioned. For example, $A_3C_{60}$ and $Na_2AC_{60}$ ($A$ = K, Rb), which have similar structures but different orientational states, are both superconducting but with a different dependence of the transition temperature on the lattice parameter [2,3]. In the $(AC_{60})_n$ polymers, different orientations in $C_{60}$ chains might control a transition between 1D and 3D electronic structures [4]. In tetrakis-dimethylamino-ethylene (TDAE)-$C_{60}$, the orientational order can be changed by the cooling process, which results in different magnetic ground states [5]. Nevertheless, the correlation between electronic properties and orientations has remained difficult to pinpoint. Recently, we have resolved the dispersion of a band in a $C_{60}$ monolayer through angle-resolved photoemission spectroscopy (ARPES) [6], which opens the possibility to monitor directly the changes in band structure as a function of orientations. A high sensitivity of the band structure to relative molecular orientations can be expected because the three degenerate lowest unoccupied molecular orbitals (LUMOs) that form the conduction band, which are mainly built out of $p$ orbitals pointing radially at each carbon atom, have high angular momenta ($L = 5$) [7]. We present here an ARPES study of $C_{60}$ monolayers where structural changes, including different molecular orientations, are induced by the use of two different substrates, Ag(111) and Ag(100). We evidence a complete change of symmetry of the Fermi surface (FS) and of the band dispersion, and investigate the role of orientations in the electronic structure with first-principles band-structure calculations for some of the configurations encountered in these monolayers.

The growth of $C_{60}$ monolayers on different substrates is very well documented [8]. We first deposited a $C_{60}$ multilayer onto a clean Ag substrate and obtained a monolayer by annealing it at ~650 K, then we doped the layer by potassium (K) evaporation. The cleanliness of the substrate was checked by the observation of Ag surface states [9], which disappear after $C_{60}$ deposition. The structure of the monolayer results from a compromise between the $C_{60}$ substrate and $C_{60}$-$C_{60}$ interactions, which are of similar strength on noble metal surfaces [8]. The Ag(111) surface offers the best lattice match with $C_{60}$, leading to a hexagonal $C_{60}$ overlayer, very similar to a (111) plane of the bulk compounds. In case of Ag(100), the hexagonal packing of $C_{60}$ is distorted along one of the two equivalent directions, as illustrated in Fig. 1(a). While this structure has first been described as $c(6^*4)$ [10], an incommensurate

  

structure was proposed more recently [11]. For our monolayer, the low energy electron diffraction (LEED) pattern, presented in Fig. 1b, is in better agreement with $c(6^*4)$, although some distortion from this model structure might be present. As for the $C_{60}$ orientation on top of the Ag(100) substrate, the scanning tunneling microscopy (STM) [12] and the x-ray photoelectron diffraction (XPD) [13] reveal the coexistence of two orientations, with either a single (5-6) bond (between a pentagon and a hexagon) or a double (6-6) bond (between two hexagons) facing the substrate and being aligned with the [110] or [1-10] direction [see examples on Fig. 1(a)]. These orientations contrast with most noble metal (111) surfaces where a hexagon of $C_{60}$ faces the substrate [14], as for Ag(111) [15].

The main ARPES results of the present study are summarized in Fig. 2, which compares the electronic structure of two monolayers. In both cases, the number of electrons per $C_{60}$ is estimated from the integrated area of the LUMO peak to be near three, i.e., the band is half filled. All data were collected at the Advanced Light Source with a 35 eV photon beam in grazing incidence and polarized nearly perpendicularly to the sample surface [6]. In the top of Fig. 2, we show with dotted lines the contour of the FS that reflects the different symmetry of the structure of the $C_{60}$ monolayers, induced by the substrate. The FS is almost circular in the case of $C_{60}$/Ag(111), while it is rather rectangular for $C_{60}$/Ag(100). The complete analysis of the FS symmetry was given in ref. [6] for Ag(111) and will be given below for Ag(100). In the bottom of Fig. 2, we further compare the dispersion along high symmetry lines, which reveal a more unexpected contrast. Most notably, the $\Gamma$ point is unoccupied in $C_{60}$/Ag(111), while it is occupied for at least one of the three LUMO sub-bands in $C_{60}$/Ag(100). As the $\Gamma$ point is common to the two $C_{60}$/Ag(100) domains, this behavior directly establishes a significant difference in band structures, regardless of any further analysis or structural details. We argue below that this change is related to the different orientations.

Figure 3 presents a larger view of the reciprocal space in the case of the Ag(100) substrate. The map was obtained by integration of the spectral intensity between 0.01 and $-0.05$ eV from the Fermi level ($E_F$). As a result of the molecular nature of $C_{60}$-based compounds, the photoemission cross sections are strongly energy and angle dependent [16], and particular attention has to be given to the meaning of the measured intensities. Here, dispersion images show that each high intensity region of the map corresponds to a band dispersing towards $E_F$, like in Fig. 2. This rules out a simple modulation of the intensity due to cross section or photoelectron diffraction effects [17]. Furthermore, the map presents the periodicity of the $C_{60}$ reciprocal lattice, whereas such modulations would be expected over a much larger angular range. The determination of the FS is complicated in Ag(100) by the presence of two domains, but their respective contribution can be distinguished by sampling a large area of momentum space, as in Fig. 3, because this covers many Brillouin zones (BZ) with inequivalent contributions from the two domains. The map is characterized by a clear symmetry with respect to the diagonals (black dashed lines), which is actually expected from the superposition of the two domains (see inset at left of Fig. 3). Furthermore, the high intensity regions (yellow

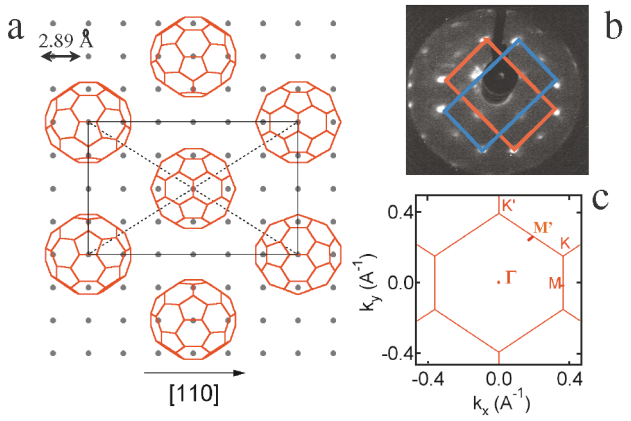


FIG. 1 (color). (a) Sketch of the $C_{60}$/Ag(100) structure with respect to the positions of Ag atoms (grey points). $C_{60}$ are drawn with the two possible orientations: hexagon-hexagon (6-6) double bond or pentagon-hexagon (5-6) single bond on top. (b) LEED for the $C_{60}$/Ag(100) monolayer at 14 eV. Red and blue rectangles define the reciprocal unit cell for the two domains. (c) Sketch of the first Brillouin zone and location of high symmetry points.

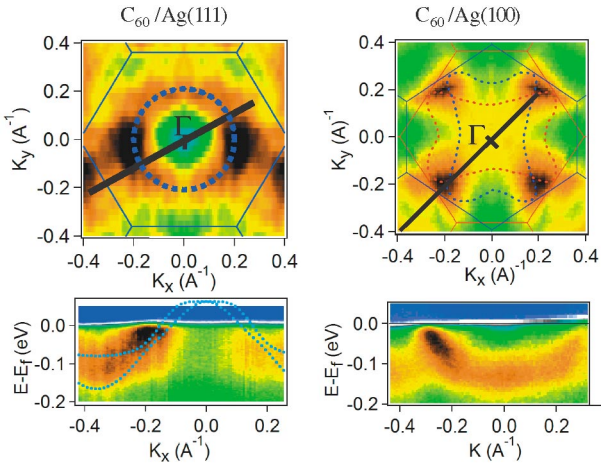


FIG. 2 (color). Comparison of $C_{60}$/Ag(111) and $C_{60}$/Ag(100) monolayers near half filling. Top: Map of the spectral intensity at the Fermi level in the first BZ (see Fig. 3 for color scale). The dotted lines locate the FS, defined by Fermi level crossings on dispersion images. For Ag(111), asymmetry in the intensity distribution is due to matrix element effect. For Ag(100), red and blue contours refer to the two domains and are determined through the analysis of Fig. 3 (see text). Bottom: Dispersion along the direction indicated by the thick black line on the map above.

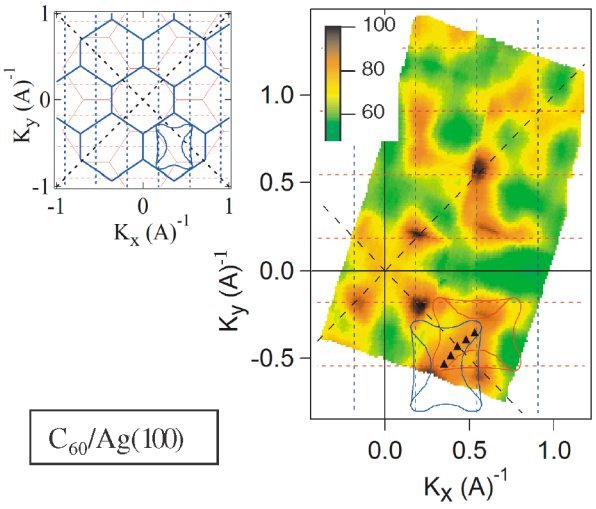


FIG. 3 (color). Fermi surface map for the $C_{60}/Ag(100)$ monolayer near half filling. No symmetry operation was applied to the data. Inset (left): Brillouin zones for the two domains (red and blue) showing the position of the dotted lines describing the location of the Fermi surface (see text). Black triangles: Fermi level crossings for one sub-band.

to black color) are concentrated along regularly spaced vertical and horizontal lines, shown in Fig. 3 as blue and red dotted lines, respectively. As there is no fourfold symmetry for one domain, this regular pattern must originate from a well-defined axial symmetry within each domain, which will appear as a squaring after superposition. There are two symmetry axes in the BZ that could play this role, $\Gamma M$ and $\Gamma K'$ [see Fig. 1(c)], but the spacing between the dotted lines is only consistent with segments oriented along $\Gamma K'$. This means that the vertical segments of high spectral intensity arise from the domain drawn in blue, and the horizontal ones from the one in red. For each domain, the dotted lines define a "stripe", reported on the inset of Fig. 3, which must contain most of the FS boundaries.. It can be worked out that it is the overlap between the bands of the two domains that blurs the intensity at $E_F$ in some regions of the map (e.g., along the blue line at $k_y = 0$).

The clarity of the square pattern implies a simple Fermi surface geometry, which is in fact surprising when one considers that the $C_{60}$ LUMOs are triply degenerate, suggesting more than one piece of FS. To create a simple pattern, all LUMO-derived sub-bands must have similar FS contours mostly following the dotted lines. In fact, we could only distinguish sub-bands if and/or when their FS contours deviate from the dotted lines. There is such a region near ($k_x = 0.4$, $k_y = -0.4$), indicated by black triangles. The dispersion image at $k_y = -0.4$ Å$^{-1}$ (not shown) reveals two bands crossing the Fermi level with opposite slopes. This allows us to refine the contour of the FS for these two different sub-bands and the result is shown in Fig. 3. The larger, more rectangular, contour corresponds to one (or possibly two) sub-band(s) empty at $\Gamma$, while $\Gamma$ is filled for the other contour and corresponding band(s). For clarity, we have reported only the average contour of these two pieces of Fermi surface in Fig. 2.

With this knowledge about the FS of $C_{60}/Ag(100)$, we can return in more details to the comparison of Fig. 2. For $C_{60}/Ag(111)$, the monolayer is a single domain and all directions look roughly the same due to the high hexagonal symmetry. The comparison with the theoretical band structure indicates that the observed dispersion corresponds to two unresolved sub-bands and that the third one remains totally empty [6]. For $C_{60}/Ag(100)$, we present the dispersion along the diagonal, where it is the clearest because it is nearly the same direction, roughly corresponding to $\Gamma M'$, in both domains. In addition to the difference in curvature at $\Gamma$, it is interesting to note that the dispersion is significantly larger for Ag(100) compared to Ag(111), namely, 135 meV ± 15 meV compared to about 100 meV. Naively, one would expect the opposite because the distances between $C_{60}$ are larger on Ag(100) than Ag(111), which should reduce the bandwidth. This further proves that the band structure is not simply "rescaled" according to the new lattice but much more deeply modified and that all parameters must be considered before comparing two different $C_{60}$ systems.

Two factors come to mind to explain the change in band structure, either the interaction with the substrate or the orientations of the $C_{60}$ molecules. It is difficult to estimate a possible contribution from the substrate, but the electronic structure for the K-doped $C_{60}/Ag(111)$ monolayer was found to be very similar to that of the bulk [6], suggesting only a marginal influence, as also concluded in Ref. [18] for doped monolayers on noble metal surfaces.

To get a better understanding of the possible role of the orientations, we now take a closer look at the contact geometry between two neighboring molecules in the different cases. On Ag(111), the contact is always through two single bonds, as sketched in (A) of Fig. 4. Note that this ordering of the $C_{60}$ molecules is very close to that

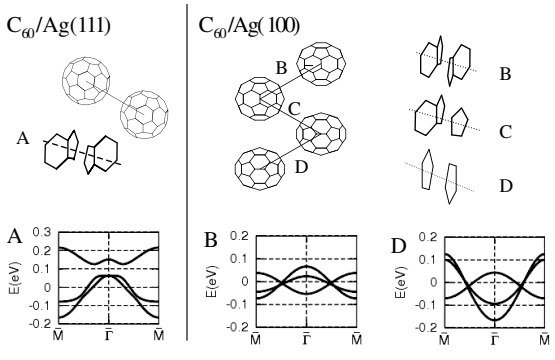


FIG. 4. Top: Sketch of the relative positions of the first carbon neighbors for different $C_{60}$ arrangements. The dotted line joins the center of the two neighboring molecules. Bottom: First principle band-structure calculations for some of the configurations shown above.

found in the (111) plane of the disordered fcc structure of $A_3C_{60}$. On Ag(100), more different contact geometries are encountered, depending on the respective orientations of two neighboring molecules. A molecule oriented along a 6-6 bond on top can present either a single bond or a pentagon to its neighbor. This results in three possible contact geometries, for this 6-6 orientation only (see Fig. 4): two single bonds face to face (B), a single bond towards a pentagon (C), and two pentagons face to face (D). To investigate the impact of these changes on the electronic structure, we have calculated the band-structure [19] in cases B and D and found a large difference, as shown on Fig. 4, with bands reaching much lower energies at $\Gamma$ for case D. This demonstrates the ability of the orientations to change the electronic structure.

It is difficult to make a full realistic calculation for Ag(100) because of the coexistence of different orientations and also of some uncertainty in the 5-6 orientation (it differs by a few degrees between STM and XPD [12,13]). However, the previous analysis supports the idea that it is the type of contact geometry that defines the general shape of the band structure. Indeed, for cases A and B, which are in a similar (but not identical) configuration, the dispersion is minimum at $\Gamma$ for at least two bands, in sharp contrast with the very different configuration represented in D, where two bands show a high maximum at $\Gamma$. STM images show frequent alternation between different orientations, although in a random way. The structure in Ag(100) is then likely to be dominated by the "bond vs polygon" type of configuration (case C), which is obtained each time two neighboring molecules have a different orientation. In fact, this type of configuration is the most favorable energetically because an electron-rich bond faces an electron-poor polygon. This is what stabilizes the orientationally ordered simple-cubic unit cell (sc) structure [20] (that of $Na_2CsC_{60}$ at low temperatures), where four different orientations alternate in the (111) plane to create the bond vs polygon situation. We believe that it is these identical contact geometries that allow the development of a well-defined dispersive structure despite the disorder in orientations. Furthermore, our ARPES result in $C_{60}$/Ag(100) is in qualitative agreement with the calculation for the sc structure, based on these contact geometries, where $\Gamma$ is occupied for two bands [7].

In conclusion, we evidence here for the first time the impact of a change in $C_{60}$ orientations on the band structure of fullerides. We find that relative orientations can be more important in defining the band structure than the distances between molecules. Very early, calculations have suggested that the band structure could be very sensitive to relative orientations [7,21]. We present here new calculations for two different arrangements of the $C_{60}$ molecules, found in Ag(100) monolayer, which reveal differences in band structures in qualitative agreement with our experimental observation. We show that the difference in orientations observed in $C_{60}$/Ag(111) and $C_{60}$/Ag(100) closely correspond to the different arrangement of the molecules in a (111) plane of the fcc and sc structures, respectively. Then, our study gives an experimental basis to the relevance of orientations in band-structure calculations, not only for these monolayers, but also to approach real situations in the bulk, like the difference between $A_3C_{60}$ and $Na_2CsC_{60}$. More generally, this study gives an example of how the internal structure of the building block of complex systems can affect their macroscopic properties.

We would like to thank M. Grobis and X. Lu for useful discussion of their STM data. The SSRL's effort is supported by DOE's Office of Basic Energy Sciences, Division of Materials Science with Contract No. DE-FG03-01ER45929-A001. The work at Stanford was supported by ONR Grant No. N00014-98-1-0195-P0007 and NSF Grant No. DMR- 0071897. The computational work was supported by NSF Grant No. DMR00-87088 and BES's Office of the DOE under Contract No. DE-AC03-76SF00098. Computational resources have been provided by NSF at NCSA and by NERSC.

[1] O. Gunnarsson, Rev. Mod. Phys. **69**, 575 (1997).
[2] T. Yildirim *et al.*, Phys. Rev. Lett. **77**, 167 (1996).
[3] C. M. Brown *et al.*, Phys. Rev. B **59**, 4439 (1999).
[4] H. Alloul *et al.*, Phys. Rev. Lett. **76**, 2922 (1996).
[5] D. Mihailovic *et al.*, Science **268**, 400 (1995).
[6] W. L. Yang *et al.*, Science **300**, 303 (2003).
[7] N. Laouini, O. K. Andersen and O. Gunnarsson, Phys. Rev. B **51**, 17 446 (1995).
[8] For a review, see P. Rudolf in *Fullerenes and Fullerene Nanostructures*, edited by H. Kuzmany *et al.* (World Scientific, Singapore, 1996), p. 263.
[9] A. Goldman and E. Bartels, Surf. Sci. Lett. **122**, L629 (1982).
[10] A. Goldoni *et al.*, Phys. Rev. B **58**, 2228 (1998).
[11] W.W. Pai and C. L. Hsu, Phys. Rev. B **68**, 121403 (2003).
[12] M. Grobis, X. Lu and M. F. Crommie, Phys. Rev. B **66**, 161408 (2002).
[13] C. Cepek *et al.*, Phys. Rev. B **63**, 125406 (2001).
[14] R. Fasel *et al.*, Phys. Rev. Lett. **76**, 4733 (1996).
[15] A. Tamai *et al.* (to be published).
[16] J. Schiessling *et al.*, Phys. Rev. B **68**, 205405 (2003).
[17] S. Hüffner, *Photoelectron Spectroscopy* (Springer-Verlag, Berlin, 2003).
[18] B.W. Hoogenboom, R. Hesper, L. H. Tjeng and G. A. Sawatzky, Phys. Rev. B **57**, 11 939 (1998).
[19] M. L. Cohen, Phys. Scr. **T1**, 5 (1982); N. Troullier and J. L. Martins, Phys. Rev. B **43**, 1993 (1991); D. Sánchez-Portal, P. Ordejón, E. Artacho, and J. M. Soler, Int. J. Quantum Chem. **65**, 453 (1997).
[20] P. Launois, S. Ravy and R. Moret, Phys. Rev. B **55**, 2651 (1997), and references therein.
[21] E. L. Shirley and S. G. Louie, Phys. Rev. Lett. **71**, 133 (1993); M. P. Gelfand and J. P. Lu, Phys. Rev. Lett. **68**, 1050 (1992).